

Supporting Information

An Orange-Yellow-Emitting $\text{Lu}_{2-x}\text{Mg}_2\text{Al}_{2-y}\text{Ga}_y\text{Si}_2\text{O}_{12}:\text{xCe}^{3+}$ Phosphor-in-Glass Film for Laser-Driven White Light

Shisheng Lin,¹ Hang Lin,^{1,2,3*} Pengfei Wang,^{1,4} Ping Sui,^{1,4} Hongyi Yang,⁵ Ju Xu,
¹ Yao Cheng, ¹ Yuansheng Wang^{1,*}

¹ Key Laboratory of Optoelectronic Materials Chemistry and Physics, Fujian Institute of Research on the Structure of Matter, Chinese Academy of Sciences, Fuzhou, Fujian, 350002 (P. R. China)

E-mail: lingh@fjirsm.ac.cn; E-mail: ywang@fjirsm.ac.cn;

² Fujian Science & Technology Innovation Laboratory for Optoelectronic Information of China, Fuzhou, Fujian, 350108 (P. R. China)

³ State Key Laboratory of Structural Chemistry, Fuzhou, Fujian, 350002 (P. R. China)

⁴ College of Chemistry and Materials Science, Fujian Normal University, Fuzhou, Fujian, 350007 (P. R. China)

⁵ Xiamen Institute of Rare-earth Materials, Haixi Institutes, Chinese Academy of Sciences, Xiamen, Fujian, 361000 (P. R. China)

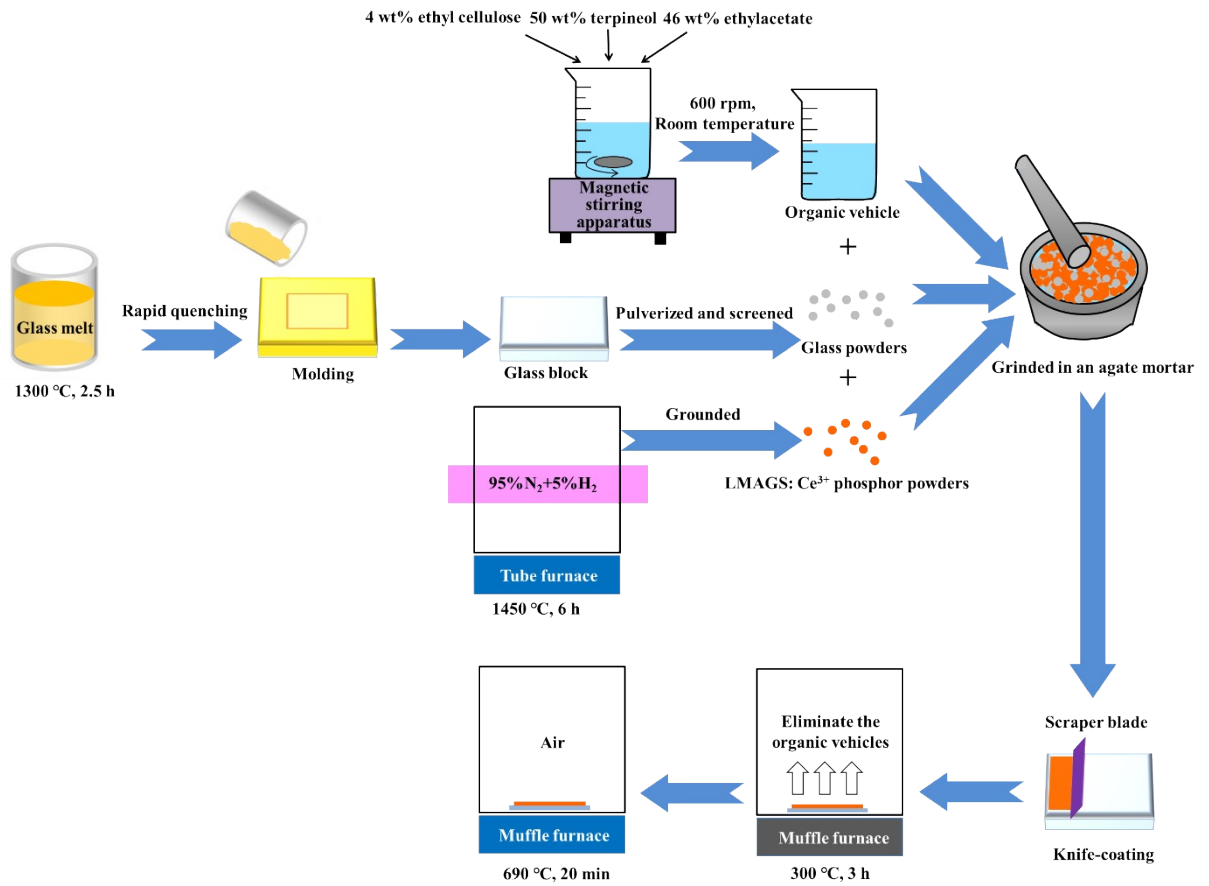


Figure S1. Schematical illustration of preparation procedure of the LMAGS: Ce³⁺ PiG film-on-SP.

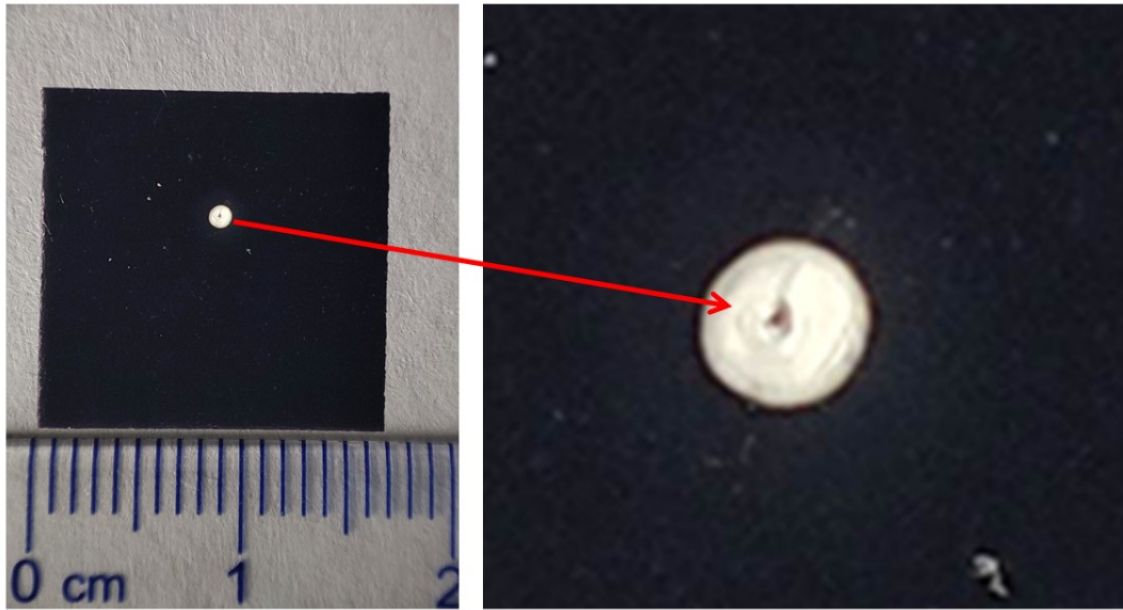


Figure S2. Photograph of the photo-sensitive paper upon blue laser irradiation

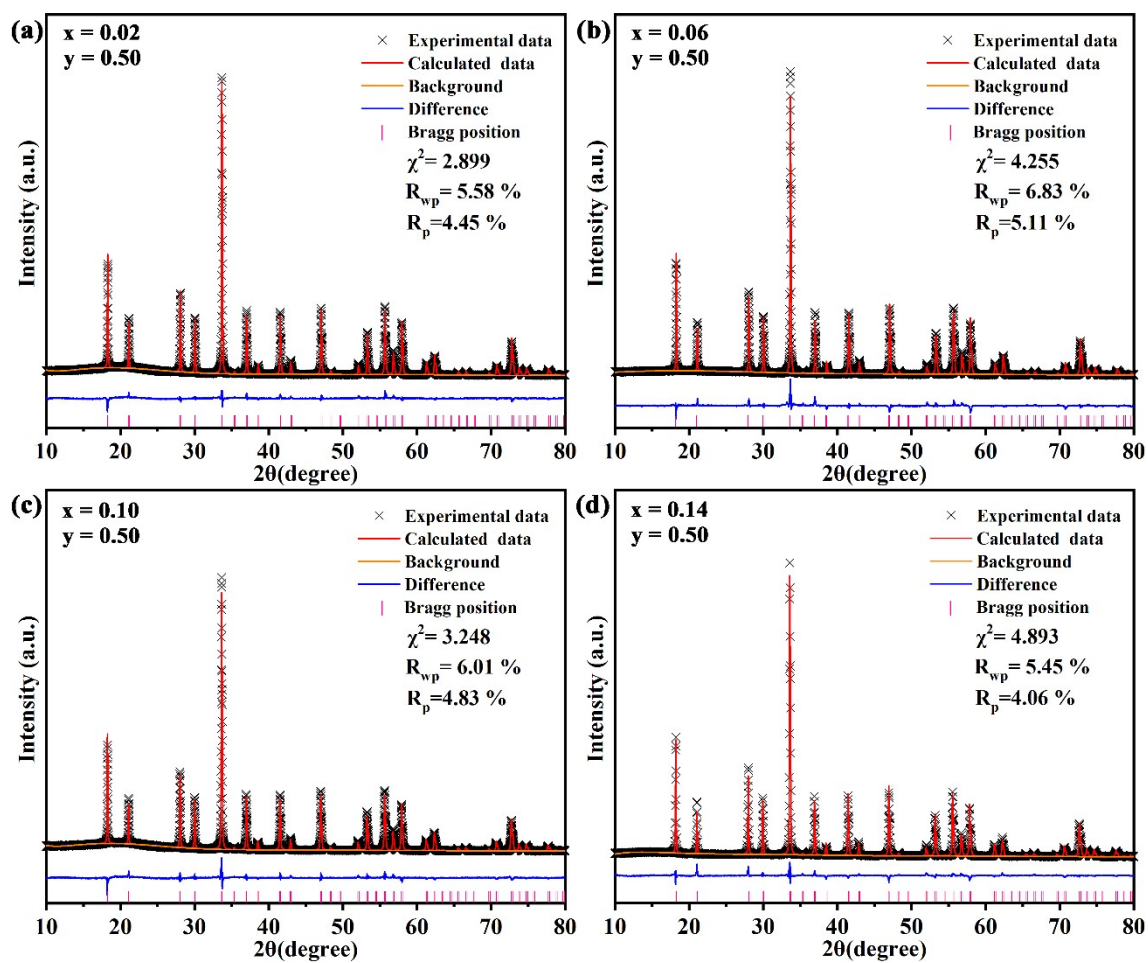


Figure S3. Rietveld refinement on Lu_{2.0-x}Mg₂Al_{1.5}Ga_{0.5}Si₂O₁₂: xCe³⁺ phosphor, showing the observed (black crosses) and calculated (red line) XRD profiles, and the difference between them (blue line).

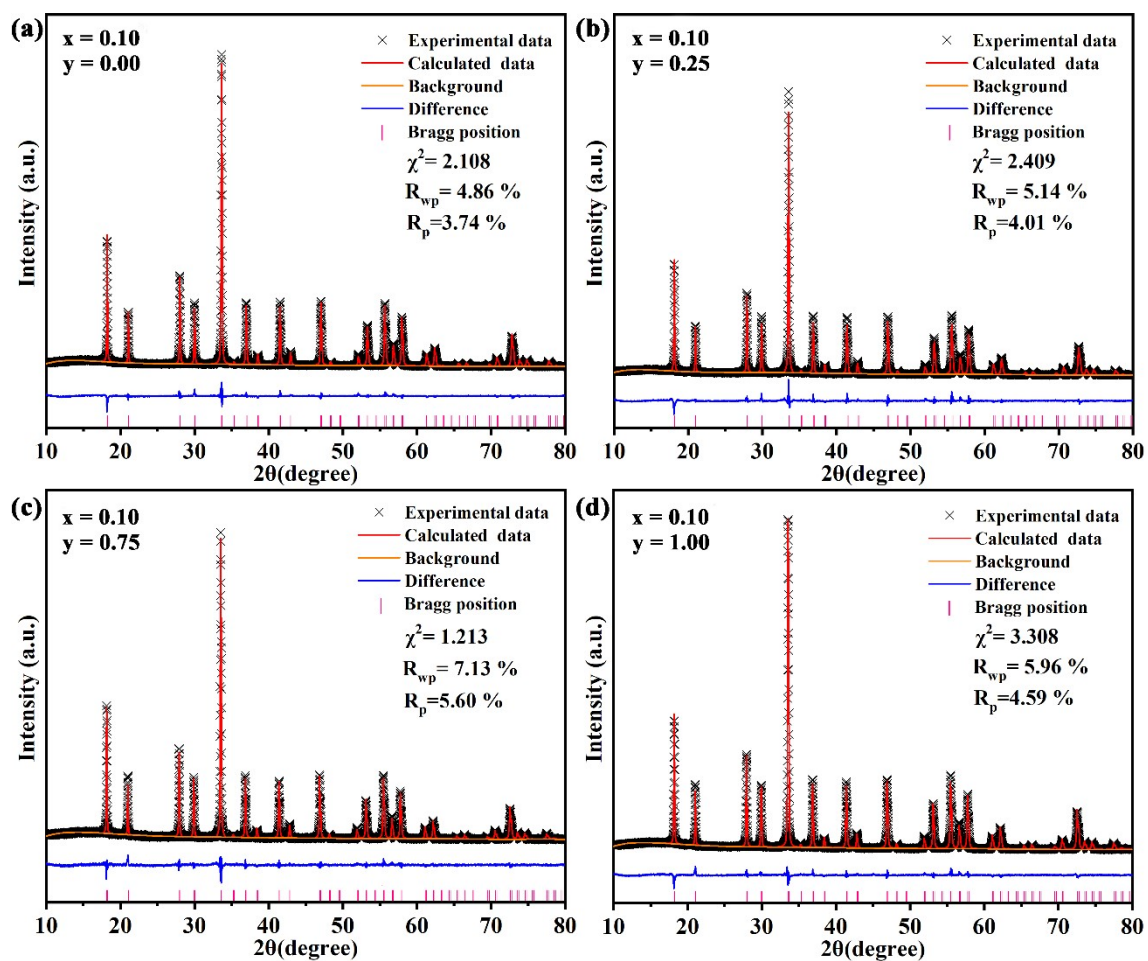


Figure S4. Rietveld refinement on $\text{Lu}_{1.9}\text{Mg}_2\text{Al}_{2.0-y}\text{Ga}_y\text{Si}_2\text{O}_{12}: 0.1\text{Ce}^{3+}$ phosphor, showing the observed (black crosses) and calculated (red line) XRD profiles, and the difference between them (blue line).

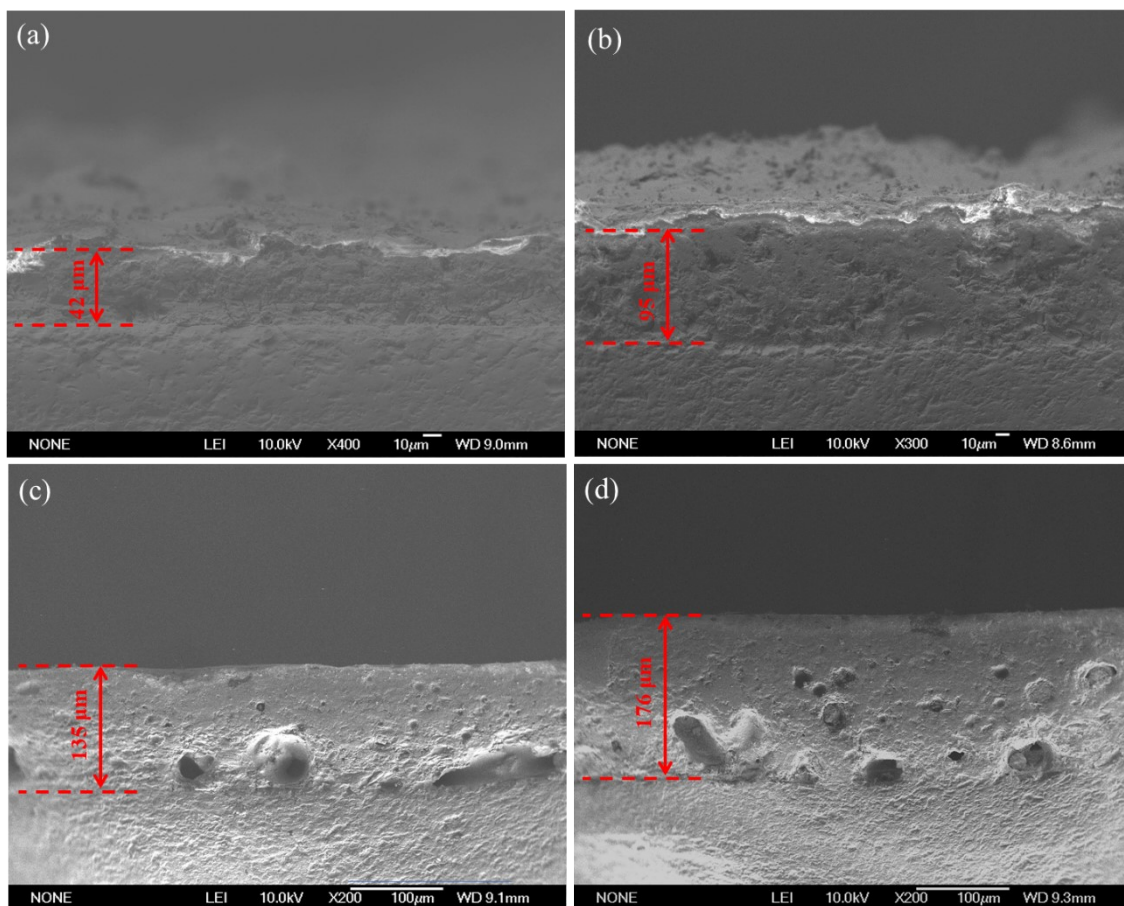


Figure S5. SEM observations on the cross section of LMAGS: Ce³⁺ PiG film-on-SP with different film thickness.

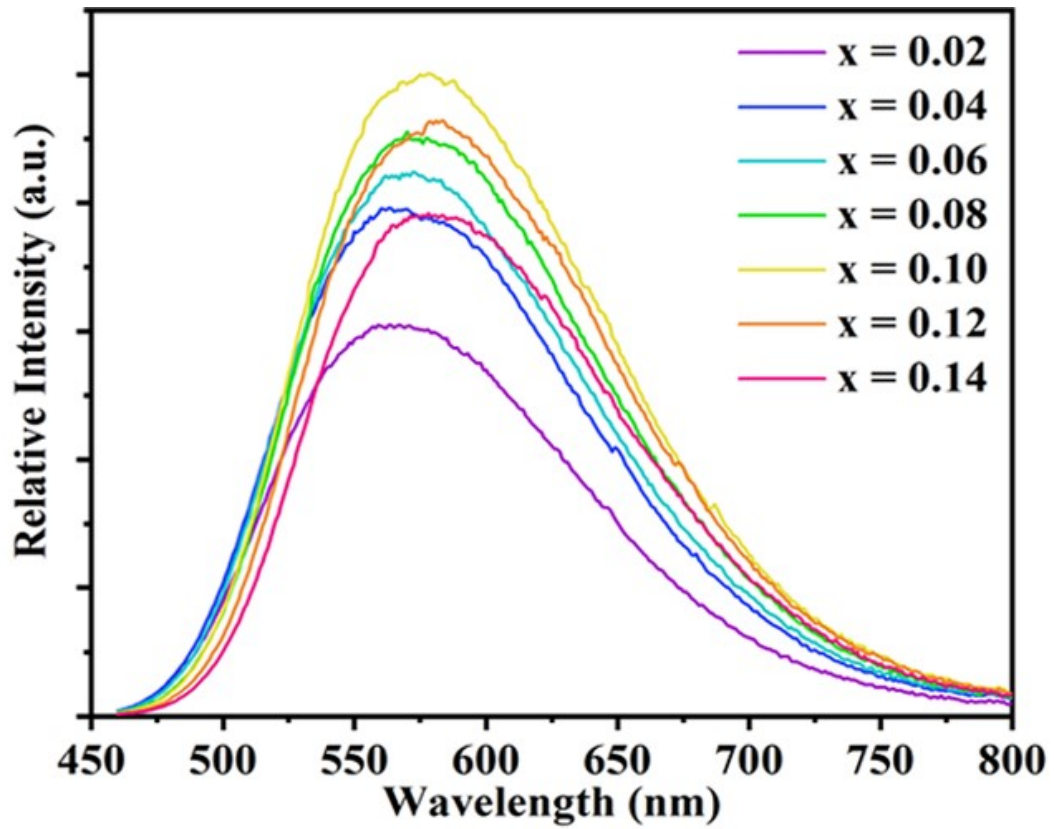


Figure S6. PL spectra of $\text{Lu}_{2.0-x}\text{Mg}_2\text{Al}_{1.5}\text{Ga}_{0.5}\text{Si}_2\text{O}_{12}: x\text{Ce}^{3+}$ PiG film-on-SP under 450 nm excitation.

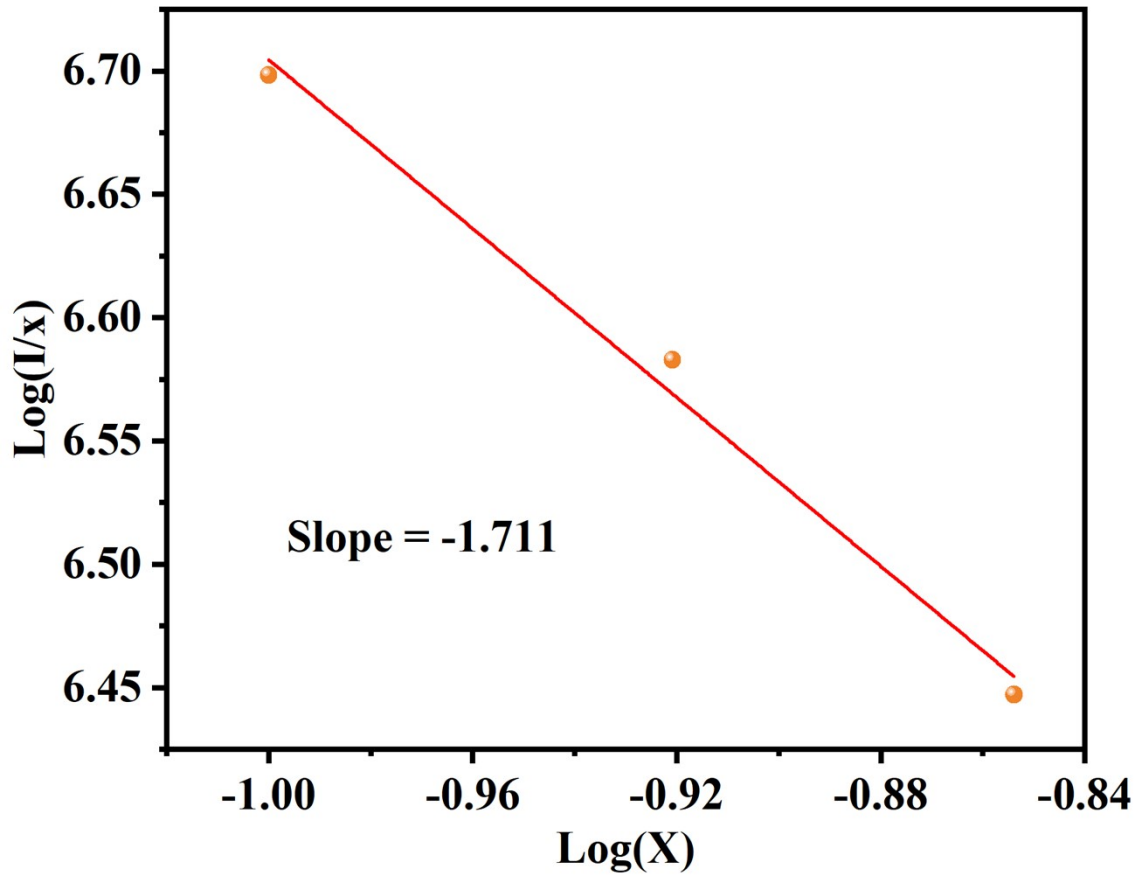


Figure S7. Relationship between $\log(x)$ and $\log(I/x)$ in the $\text{Lu}_{2.0-x}\text{Mg}_2\text{Al}_{1.5}\text{Ga}_{0.5}\text{Si}_2\text{O}_{12}: x\text{Ce}^{3+}$ phosphor.

Discussions on Figure S7:

In order to study the concentration quenching mechanism, the parameter of R_c reflecting the average distance of Ce^{3+} is introduced by using the following expression [1]:

$$R_c \approx 2 \left[\frac{3V}{4\pi x_c N} \right]^{1/3} \quad (1)$$

where V is the volume of unit cell, x_c the critical concentration of activator and N the number of available sites for the dopant in a unit cell. Taken $V=1688.219 \text{ \AA}^3$, $x_c=0.10$, and $N=8$, R_c is evaluated to be $\sim 16 \text{ \AA}$. The electronic exchange interaction should be only effective at $R_c < 5 \text{ \AA}$ to achieve energy transfer among Ce^{3+} ions. As such, the electric multipolar-multipolar interaction should be the main mechanism. Then, we adopted the Dexter theory to analyze the type of multipolar-

multipolar interaction by the following equation [2]:

$$I/x = K \left[1 + \beta(x)^{\frac{\theta}{3}} \right]^{-1} \quad (2)$$

where K and β are constants, $\theta=6, 8, 10$ means the electric multipole index corresponding to the dipole-dipole (d-d), dipole-quadrupole (d-q) and quadrupole-quadrupole (q-q) interaction, respectively. By plotting $\log(I/x)$ versus $\log(x)$, θ is calculated as 5.13, indicating that the main mechanism for concentration quenching in LMAGS: Ce^{3+} is the d-d electric multipolar-multipolar interaction.

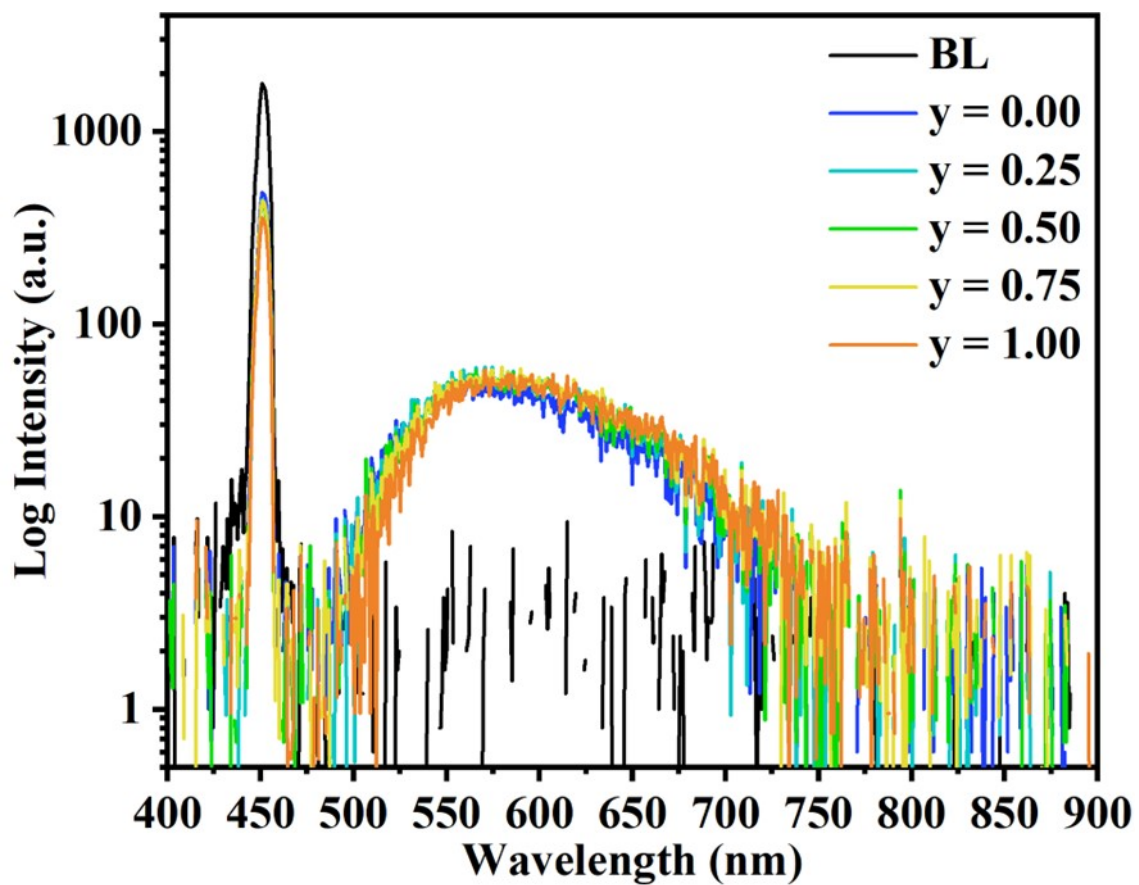


Figure S8. The measured luminescent curves of $\text{Lu}_{1.9}\text{Mg}_2\text{Al}_{2.0-y}\text{Ga}_y\text{Si}_2\text{O}_{12}: 0.1\text{Ce}^{3+}$ PiG film-on-SP to calculate quantum efficiency.

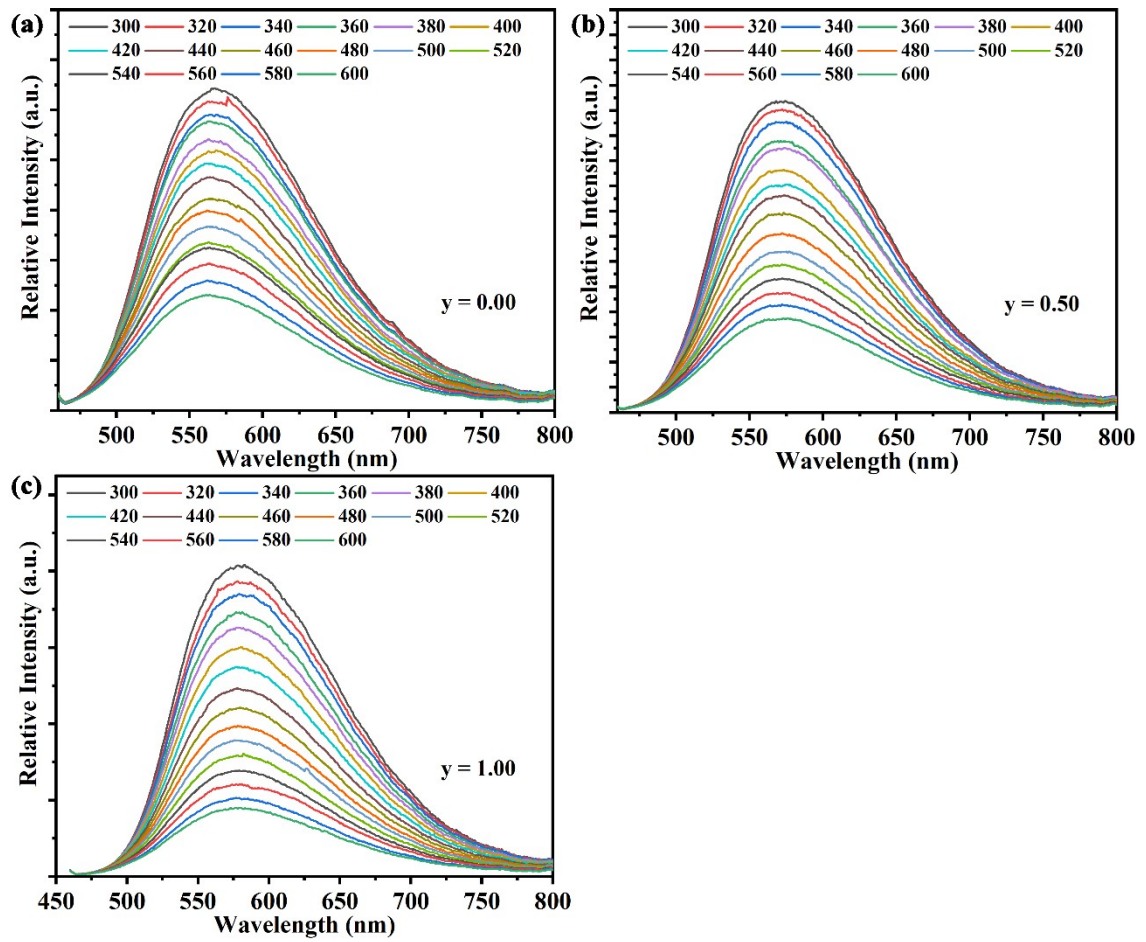


Figure S9. Temperature-dependent PL spectra in $\text{Lu}_{1.9}\text{Mg}_2\text{Al}_{2.0-y}\text{Ga}_y\text{Si}_2\text{O}_{12}: 0.1\text{Ce}^{3+}$ PiG film-on-SP from 300 to 600 K under 450 nm excitation.

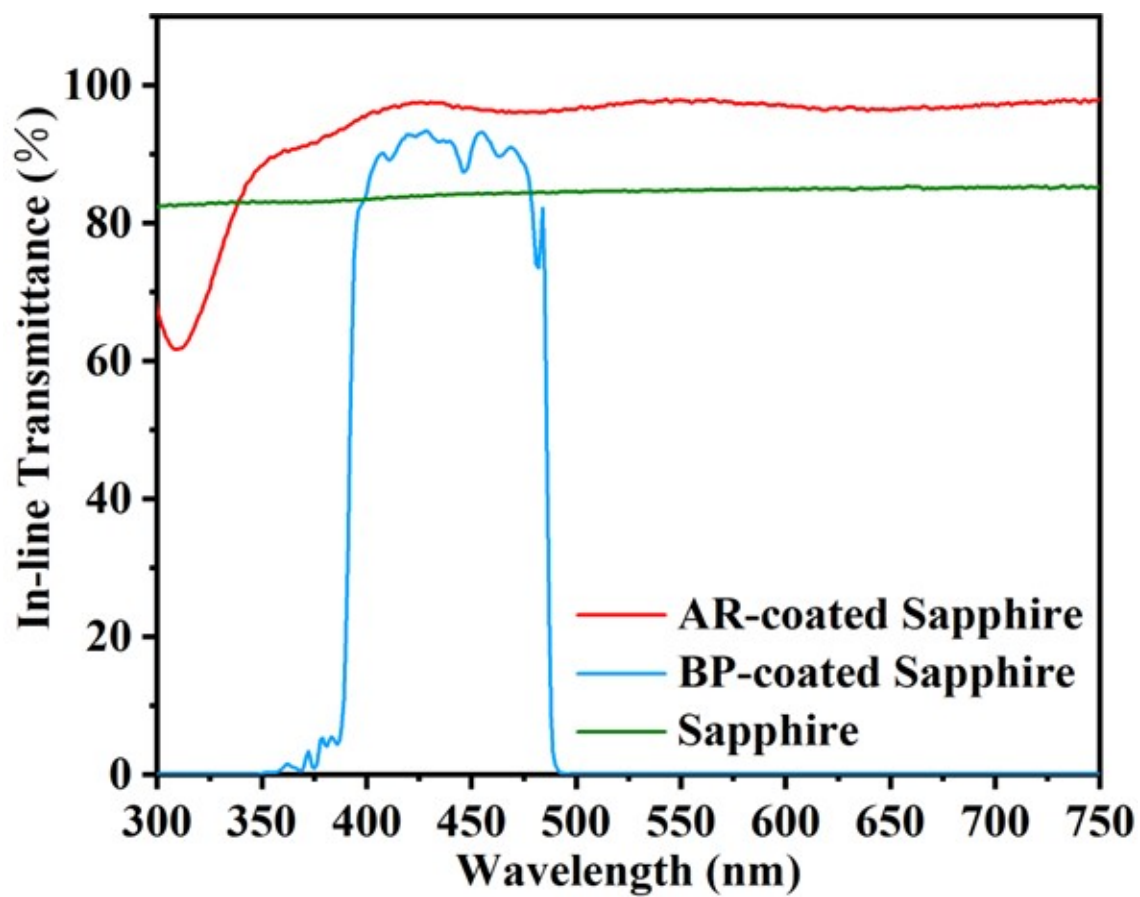


Figure S10. In-line transmittance spectra of sapphire, AR-coated sapphire and BP-coated sapphire.

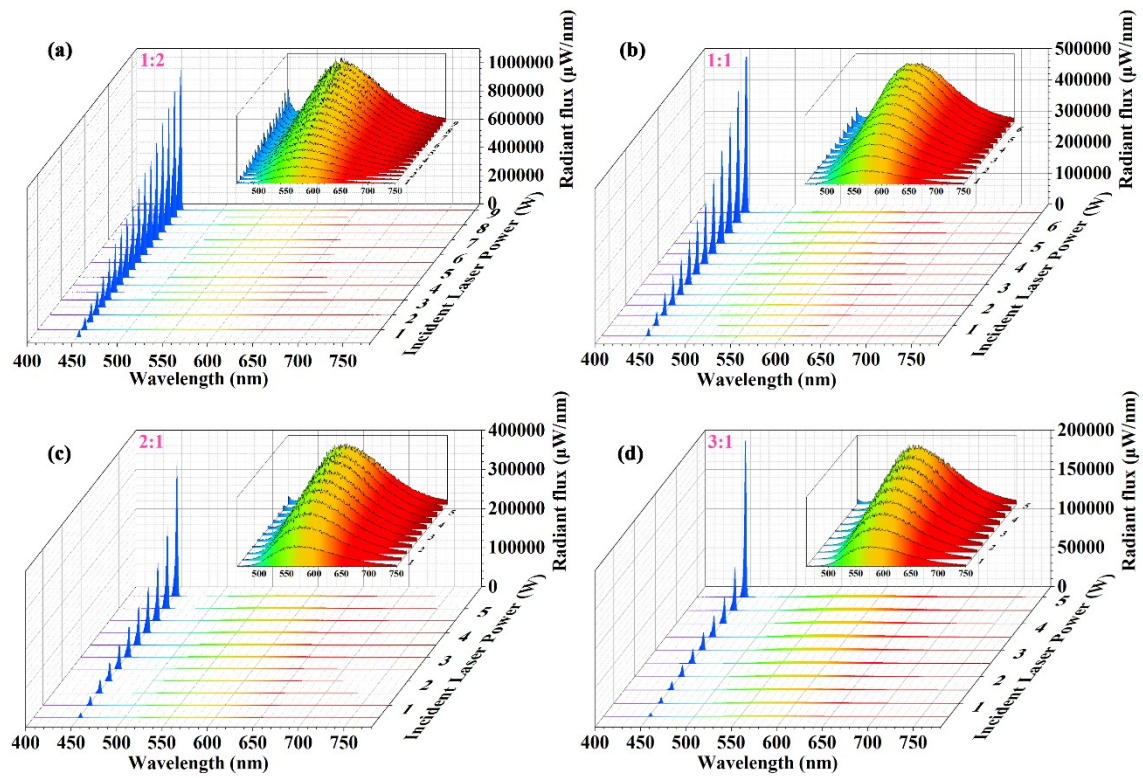


Figure S11. P_{in} dependent electroluminescent spectra of LMGs: Ce³⁺ PiG film-on-SP with different mass ratios of LMGs: Ce³⁺ phosphor to glass powders.

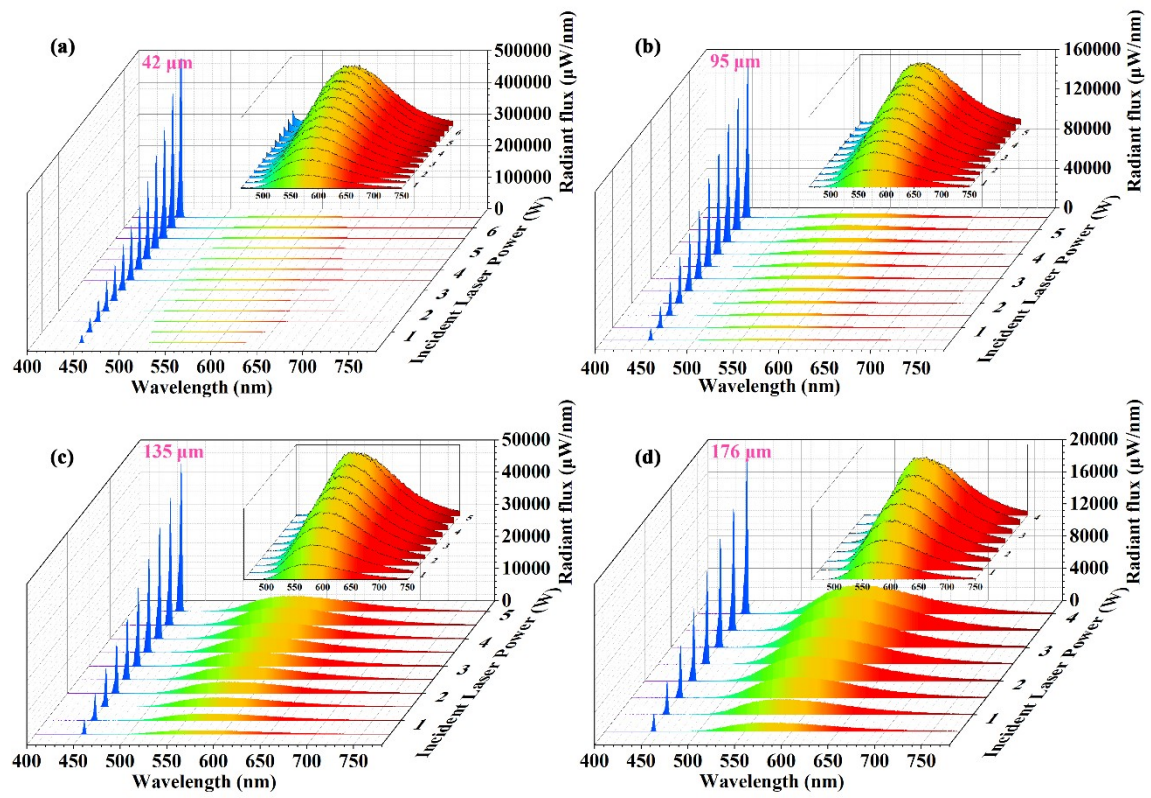


Figure S12. P_{in} dependent electroluminescent spectra of L MAGS: Ce³⁺ PiG film-on-SP with different film thickness.

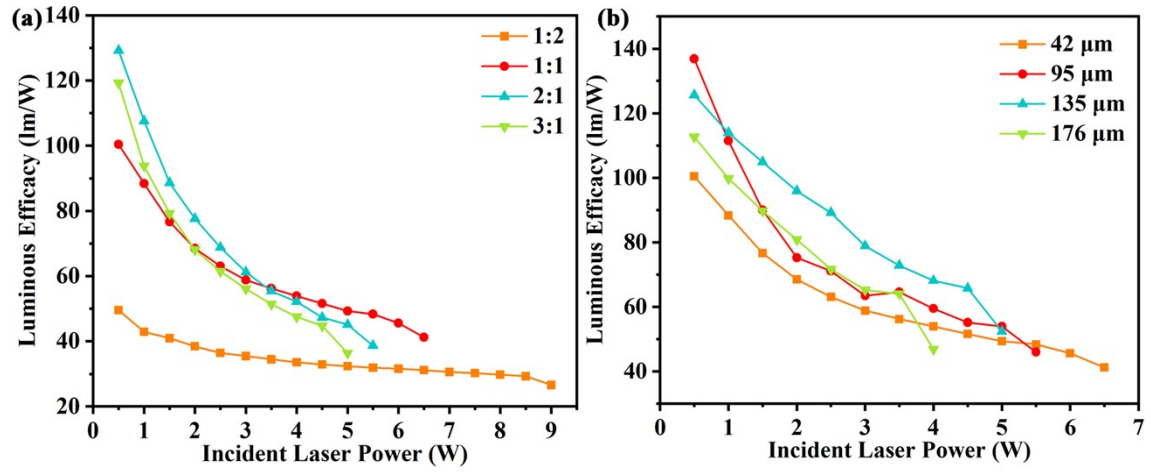


Figure S13. Pumping power dependent luminous efficacy of the LMAGS: Ce³⁺ PiG film-on-SP with (a) different weight ratios of LMAGS: Ce³⁺ phosphor to glass powders and (b) different film thicknesses.

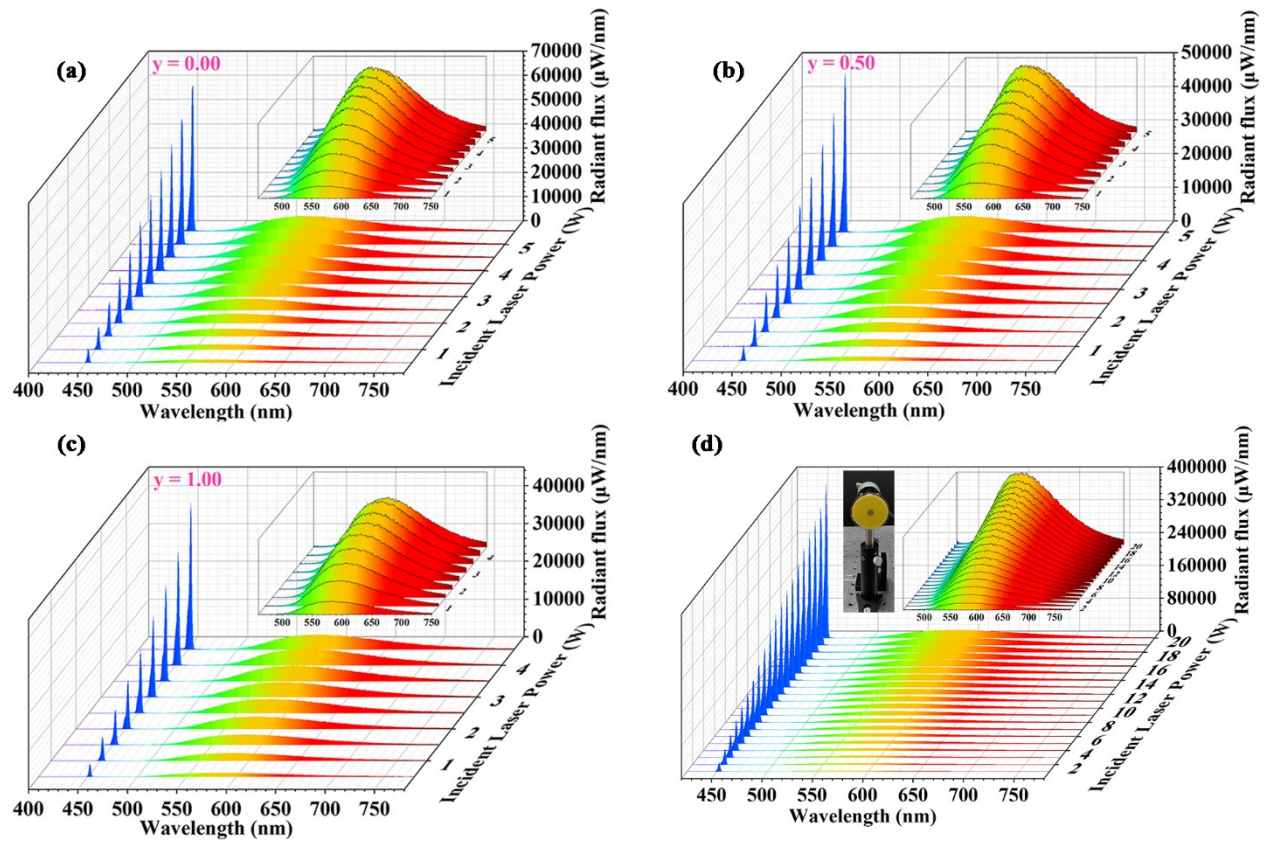


Figure S14. P_{in} dependent EL spectra of L MAGS: Ce^{3+} PiG film-on-SP with different Ga-concentration: (a) $y=0.00$, (b) $y=0.50$, and (c) $y=1.00$; insets are the corresponding magnified spectra in the range of 500-700 nm. (d) P_{in} dependent EL spectra of $Lu_{1.9}Mg_2Al_2Si_2O_{12}: 0.1Ce^{3+}$ PiG film-on-SP "phosphor wheel" measured under rotatory-reflective mode; insets are the digital photo of phosphor wheel (left) and the enlarged spectra in the region of 500-800 nm (right).

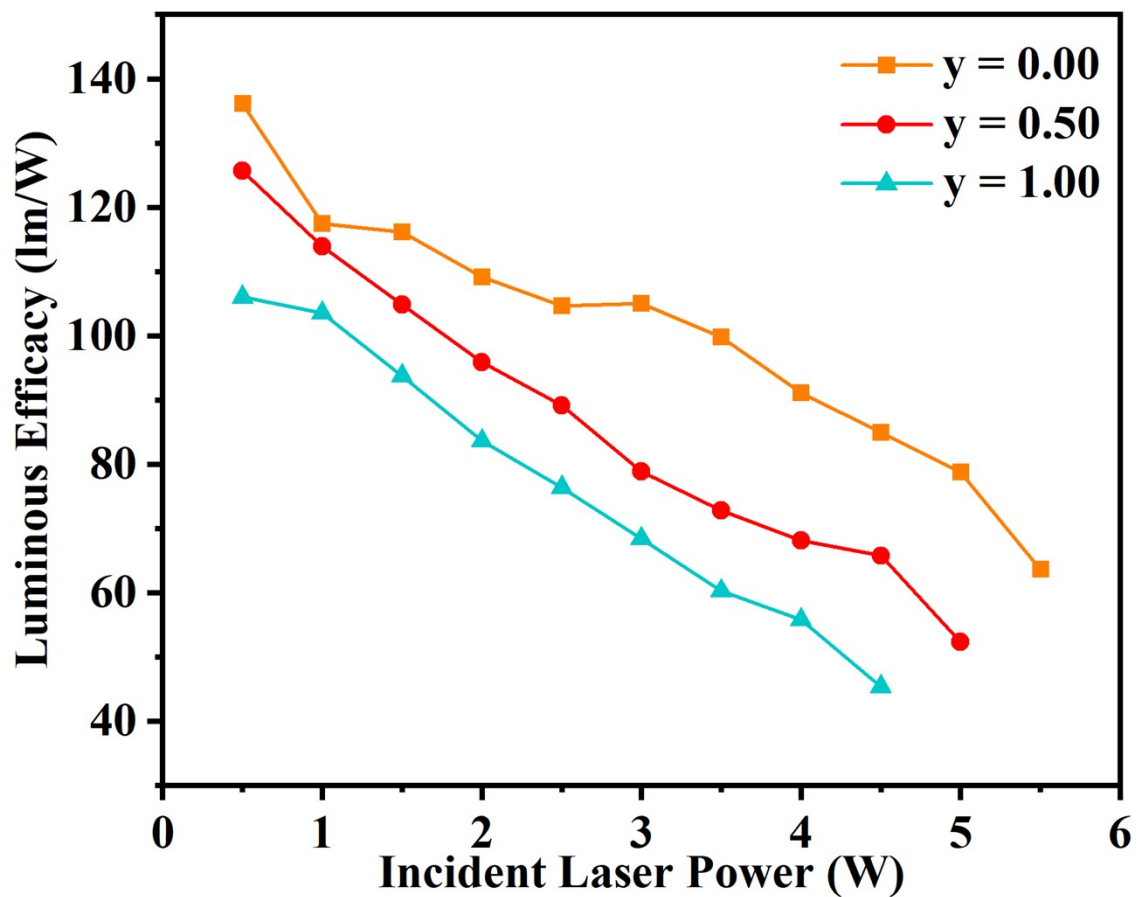


Figure S15. Pumping power dependent luminous efficacy of the LMAGS: Ce³⁺ PiG film-on-SP with different Ga-concentration.

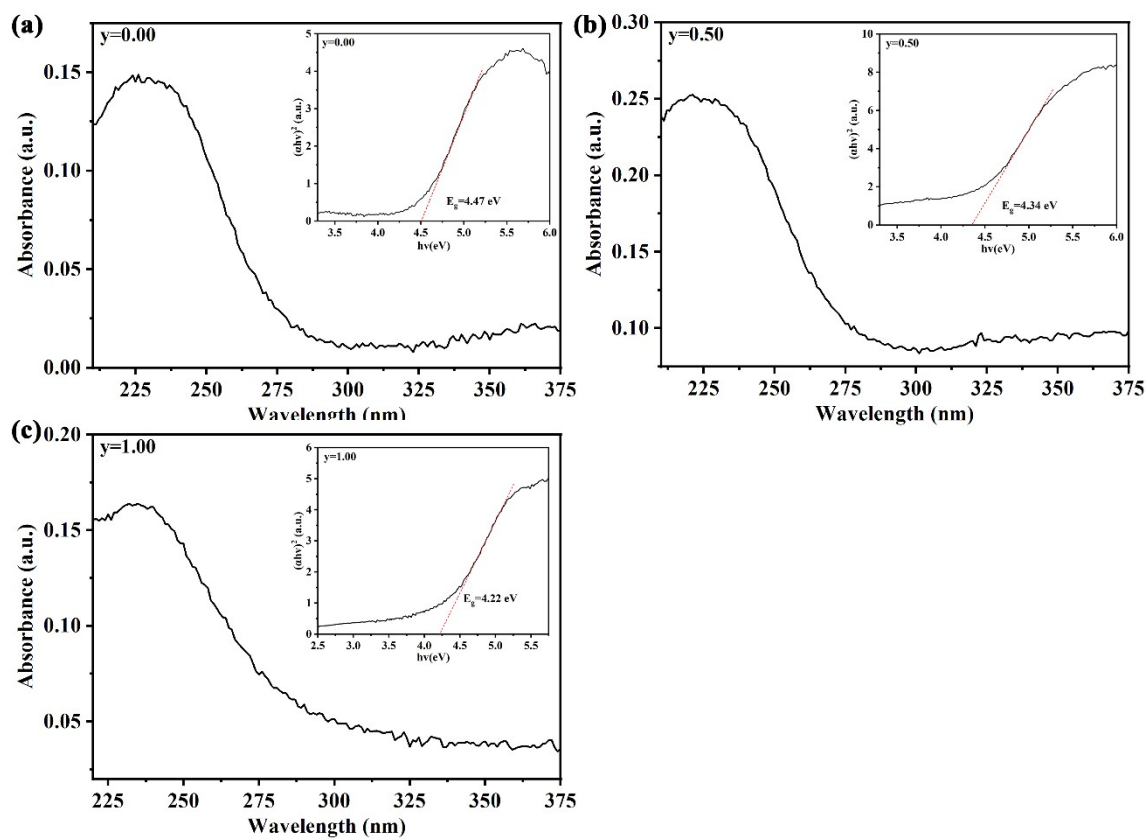


Figure S16. Diffuse-reflectance spectrum of the un-doped LMAGS, inset shows the relationship of $[ah\nu]^2$ versus photon energy $h\nu$ to determine the optical bandgap of LMAGS.

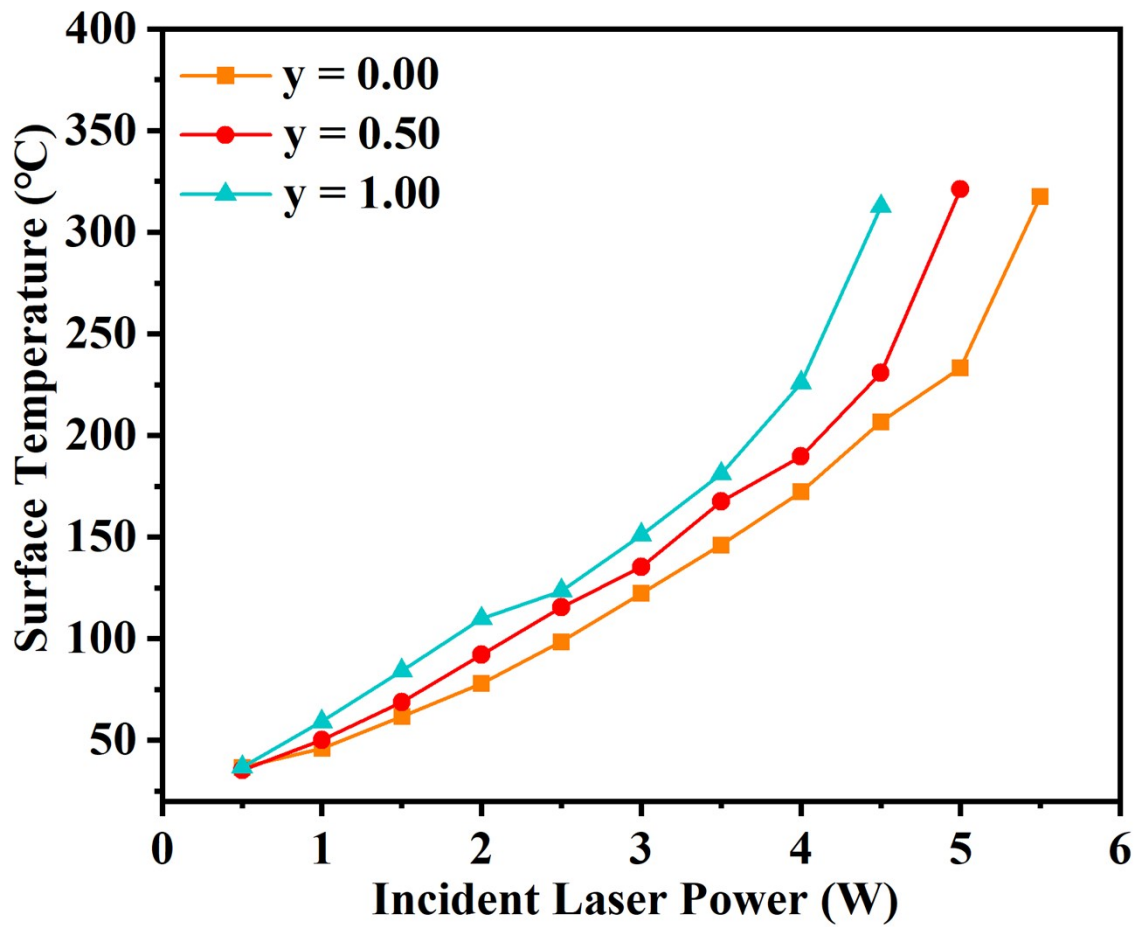


Figure S17. Local temperature of LMAGS: Ce³⁺ PiG film-on-SP with different Ga-concentration at the laser spot.

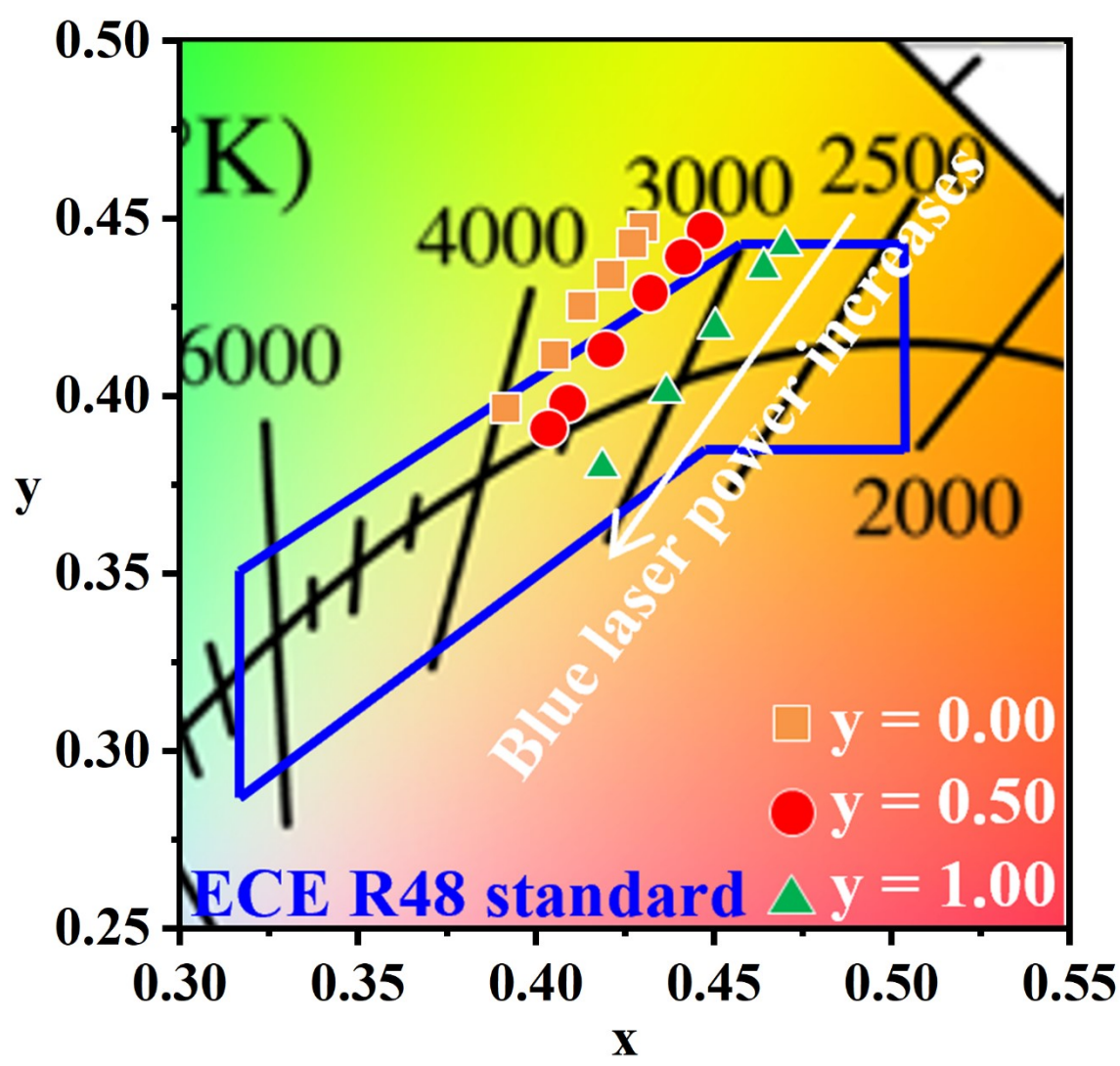


Figure S18. the variations in chromaticity coordinates of LMGs: Ce³⁺ PiG film-on-SP with different Ga-concentration.

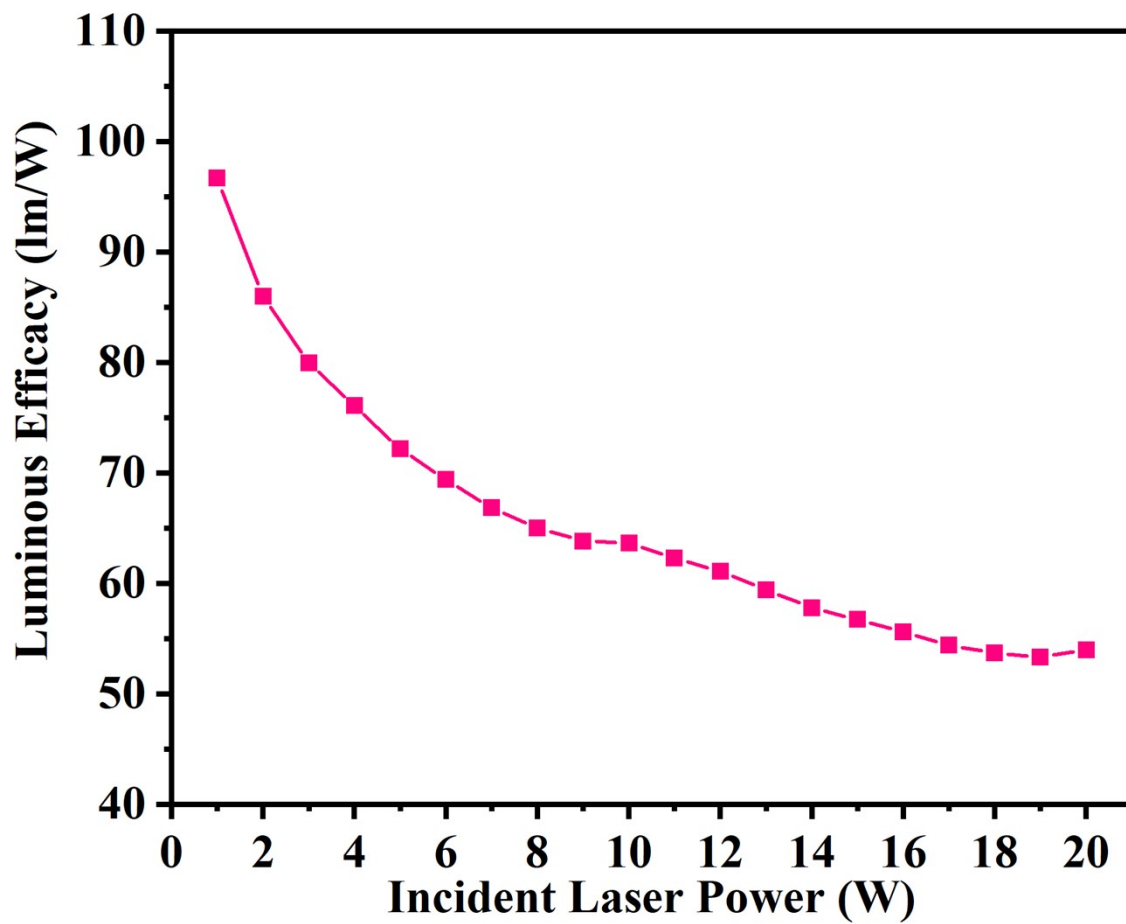


Figure S19. The derived P_{in} dependent luminous efficacy in rotatory-reflective mode.

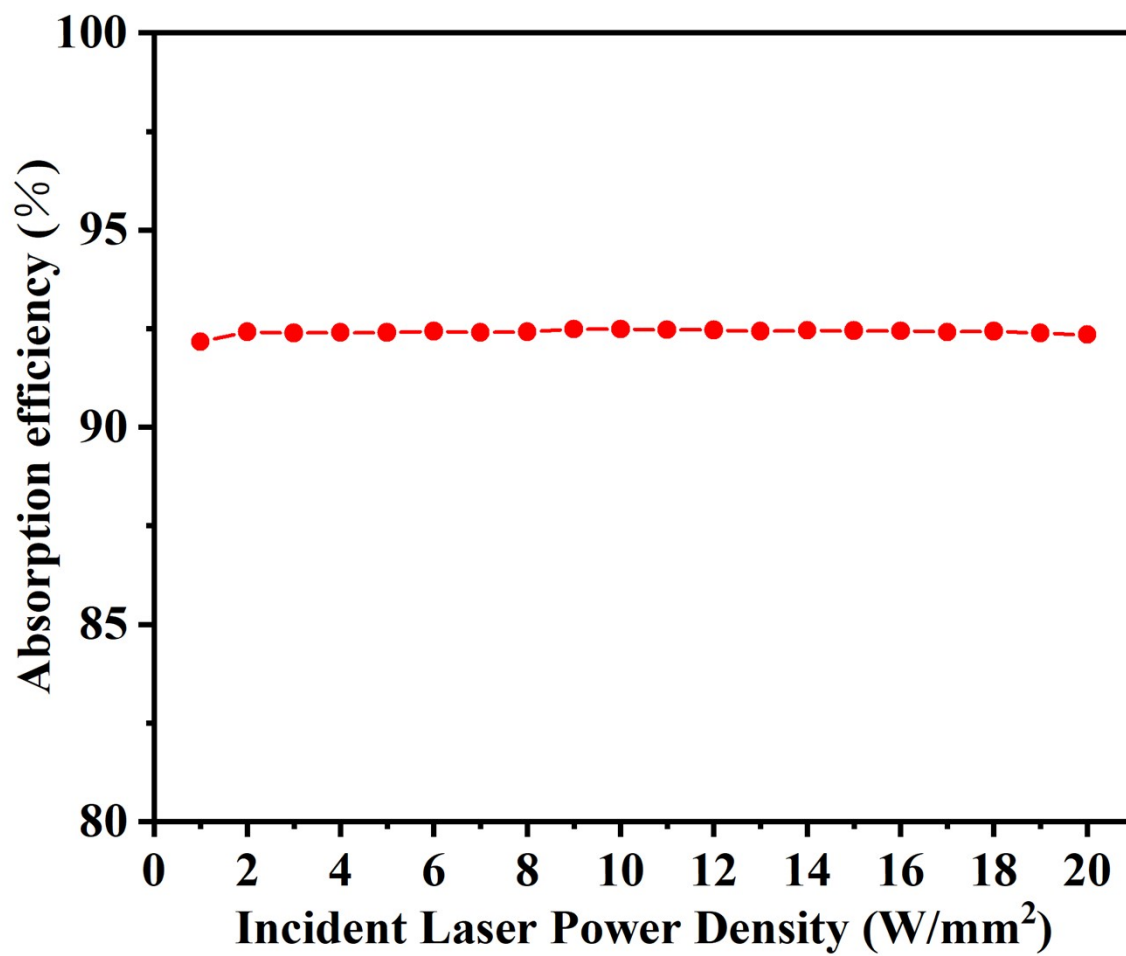


Figure S20. The incident power dependent absorption efficiencies of the LMAgS: Ce³⁺ PiG film-on-SP under rotatory-reflective mode.

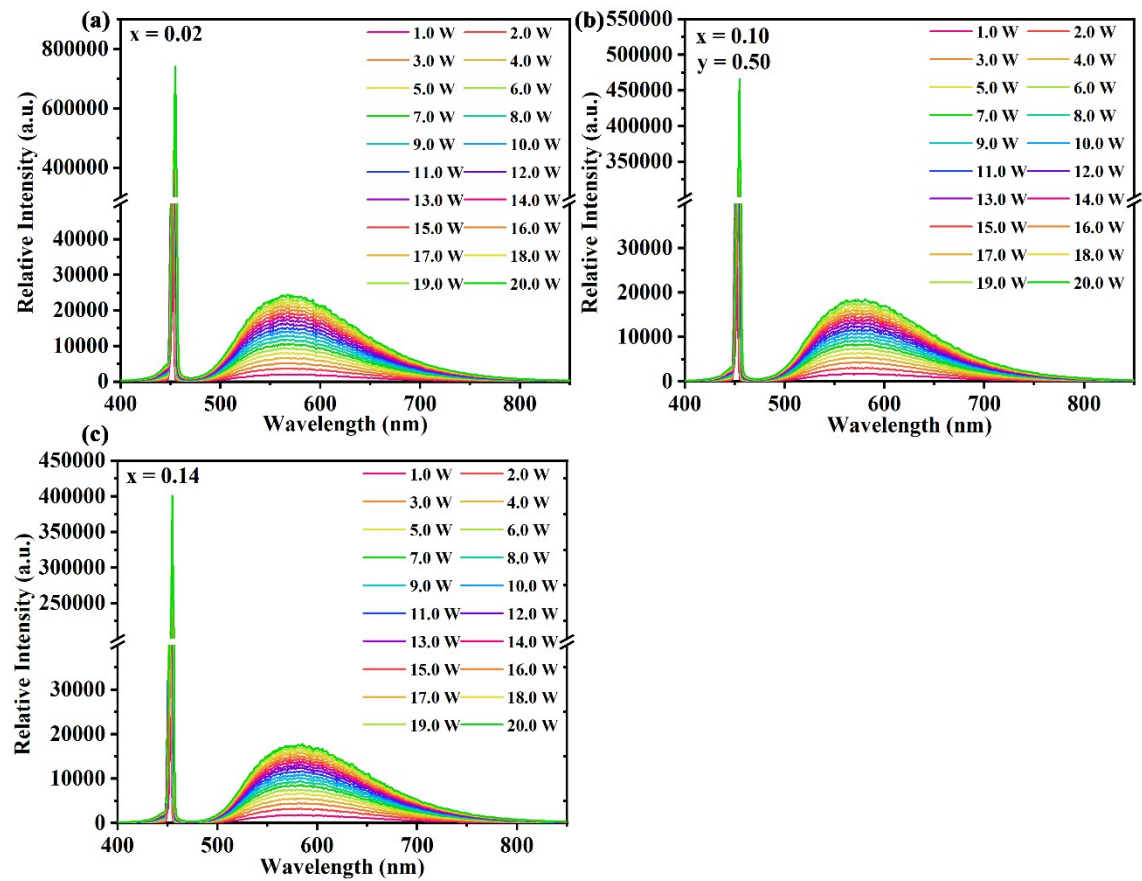


Figure S21. EL spectra of L MAGS: Ce PiG film-on-SP with different Ce-concentration under different input power density in rotatory-reflective mode.

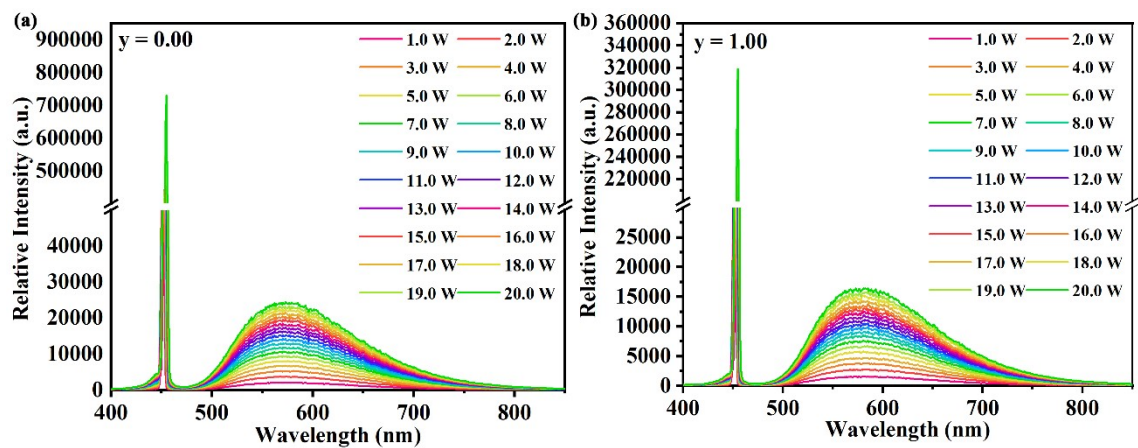


Figure S22. EL spectra of LMAGS: Ce PiG film-on-SP with different Ga-concentration under different input power density in rotatory-reflective mode.

References

- [1] G. Blasse, Luminescence of inorganic solids: from isolated centres to concentrated systems, Prog. Solid State Chem. 18 (1988) 79-171.
- [2] D.L. Dexter, A theory of sensitized luminescence in solids, J. Chem. Phys. 21 (1953) 836-850.